Article

IGBT Junction Temperature Prediction Model based on GA-LM-BP Algorithm

Yu Zhang[1,2,3,*], Tadiwa Elisha Nyamasvisva[1]

[1] Faculty of Engineering, Science and Technology, Kuala Lumpur University of Science and Technology, Kuala Lumpur, 43000, Malaysia

[2] College of Engineering Xi'an Siyuan University, Shaanxi Xi'an, 710038, China

[3] Engineering Research Centre on Additive Manufacturing Technology and Application in Universities of Shaanxi Province, Xi'an Siyuan University, Shaanxi Xi'an, 710038, China

* Email: 242924799@s.klust.edu.my

Published: 15 May 2026 | https://doi.org/10.64376/9g3swg30

Abstract: Aiming at the problem that the Insulated-Gate Bipolar Transistor (IGBT) chip is encapsulated inside the module and the chip junction temperature cannot be measured directly, an IGBT junction temperature prediction algorithm model based on the back-propagation neural network algorithm optimised jointly by the genetic algorithm and the Levenberg-Marquardt (LM) algorithm is proposed. Firstly, the temperature-sensitive electric parameter (TSEP) method is used to build an experimental platform for the saturation voltage drop of IGBT modules; then, 2250 sets of saturation voltage drop, collector current, and IGBT case temperature data are extracted from the experimental data as feature inputs to characterize their relationship with the junction temperature of the IGBT module; finally, a junction temperature prediction model is established by using the extracted electrical parameters in the Genetic Algorithm-Levenberg-Marquardt-Back Propagation (GA-LM-BP) neural network algorithm to predict the junction temperature. Finally, the GA-LM-BP neural network algorithm is used to establish a junction temperature prediction model by using the extracted electrical parameters. The experimental results show that the average absolute percentage error of the junction temperature prediction value of the GA-LM-BP neural network algorithm is 0.114 when the collector current is less than the critical current, and 0.062 when the collector current is greater than the critical current, which is more accurate than that of the GA-optimised BP neural network algorithm and classical BP neural network algorithm in predicting the junction temperature of the IGBT module.

Keywords: Insulated-Gate Bipolar Transistor (IGBT); Back Propagation (BP) Neural Network; Temperature-Sensitive Electric Parameter (TSEP); Junction Temperature Prediction Model; Genetic Algorithm-Levenberg-Marquardt-Back Propagation (GA-LM-BP) Algorithm

1. Introduction

With the continuous advancement of power semiconductor technology, insulated gate bipolar transistors (IGBTs) have been widely deployed in motor drives, high-voltage direct current transmission, renewable energy generation, and high-efficiency power conversion systems [1,2]. In practical variable-current applications, power semiconductor devices exhibit relatively high failure rates, and junction temperature is a key factor affecting the reliability of the overall power electronic system [3]. Thermal cycling and temperature ageing have been reported to accelerate degradation in power modules, and temperature-related failure mechanisms such as bond-wire fatigue and solder-layer degradation are strongly associated with junction temperature level and fluctuation characteristics [4–7]. Consequently, accurate junction temperature estimation has become a critical requirement for reliability assessment, fault prediction, and health monitoring of IGBT-based converters [7,8].

Conventional engineering practice often relies on static thermal limits or simplified thermal models provided in device datasheets, which may introduce considerable deviations under real operating conditions. To improve estimation fidelity, physics-based and electro-thermal modelling approaches, including thermal network models

with real-time temperature feedback, have been developed [9–12]. In addition, several online and non-invasive estimation techniques based on temperature-sensitive electrical parameters (TSEP) have been proposed, such as peak gate current, bus-voltage ringing, dynamic TSEP, knee voltage, voltage rise time, and turn-off diC/dt features [13–20]. However, these methods can be sensitive to modelling assumptions, device-structure variations, or operating-condition changes, which may affect robustness and general applicability [21,22].

Recently, data-driven and machine-learning-based approaches have attracted increasing attention for junction temperature estimation and prediction, including BP-neural-network-based online detection and hybrid optimisation strategies that establish nonlinear mappings between measurable electrical parameters and junction temperature [23–30]. Motivated by these advances, this paper proposes an IGBT junction temperature prediction method based on a BP neural network jointly optimised by genetic algorithm (GA) and Levenberg–Marquardt (LM) algorithms. By constructing a saturation voltage drop measurement experimental platform and extracting collector–emitter saturation voltage drop (VCE), collector current (IC), and case temperature (TC) as input features, a GA-LM-BP model is developed to achieve accurate junction temperature estimation for IGBT modules.

The main contributions of this paper are summarised as follows:

(1) An experimental platform based on the temperature-sensitive electrical parameter (TSEP) method is established to accurately characterise the relationship between saturation voltage drop, collector current, case temperature, and IGBT junction temperature.

(2) A hybrid GA-LM-BP neural network–based junction temperature prediction model is proposed, in which the global optimisation capability of the genetic algorithm is combined with the fast local convergence of the Levenberg–Marquardt algorithm.

(3) A comparative evaluation is conducted between the proposed GA-LM-BP model, the GA-BP model, and the conventional BP neural network, demonstrating the superiority of the proposed method in terms of prediction accuracy and stability under different current conditions.

2. Modelling of Junction Temperature Prediction

2.1 Establishment of the Saturation Voltage Drop Experimental Platform

A 1200 V / 75 A IGBT module is selected as the test device, and a saturation voltage drop experimental platform is constructed to characterise its electrical behaviour. The test platform mainly consists of six parts: programmable DC power supply, power load, IGBT driver board, control system, temperature control platform and oscilloscope, and the overall structure is shown in Figure 1(a). The experimental principle is shown in Figure 1(b). In this paper, the TSEP method is used to measure the saturation voltage drop without destroying the device package, and it is easy to operate.

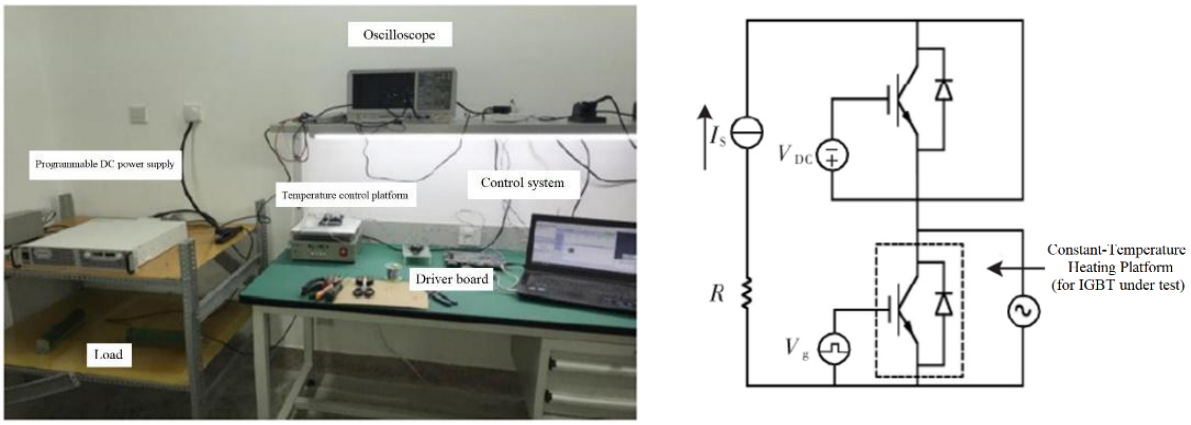

(a) Saturation Voltage Drop Test Platform (b) Saturation Voltage Drop Test Schematic

Figure 1. Test Platform of the Saturation Voltage Drop

The upper and lower tubes of the half-bridge IGBT module are connected in series, with the upper tube gate applying a negative voltage to ensure reliable shutdown, and the collector shorted to prevent false conduction; the lower tube is used as the measured object for the extraction of junction temperature-related parameters. To avoid a blind spot in the measurement of junction temperature Tj by the collector current IC due to the change of the

module's characteristics at high temperatures, the temperature gradient interval is set to be from 25°C to 150°C, and the collector current gradient interval is from 20 A to 200 A.

During the experiment, the thermostat is first set to a specified temperature, and the IGBT module is heated as a whole through the temperature control platform. After continuous heating for a long time, the IGBT reached thermal equilibrium; it can be assumed that the chip junction temperature has stabilised at the set value. Subsequently, the IGBT driver board is switched on, the signal generator is triggered with the DC power supply, and a single pulse is used to drive the IGBT to conduct briefly, and the saturation voltage drop VCE is measured simultaneously for this condition, during which the junction temperature Tj, the collector current IC, the saturation voltage drop VCE, and the enclosure temperature TC are recorded synchronously. Gradually increase the temperature and repeat the above measurements to obtain the saturation voltage drop and case temperature data under different junction temperature and collector current conditions.

The three-dimensional surface of the relationship between VCE, IC and Tj is plotted using the collected data, as shown in Figure 2. From the figure, it can be seen intuitively that VCE is affected by IC and Tj at the same time, which indicates that both VCE and IC are relevant variables associated with junction temperature variation.

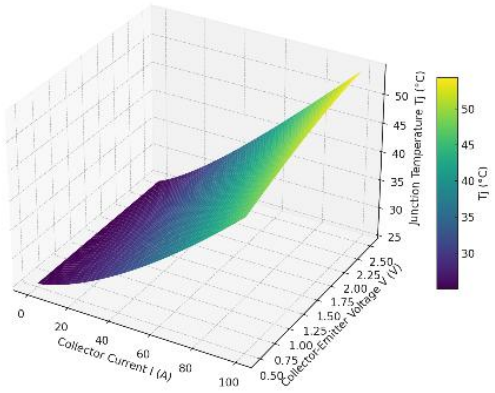

Figure 2. Three-dimensional Diagram of the Relationship among VCE, IC and Tj

2.2 BP Neural Network Prediction Model

Based on experimental data, it is difficult to clearly define the complex nonlinear relationship between the saturation voltage drop VCE, collector current IC, case temperature TC and junction temperature Tj of the IGBT. Traditional regression methods often find it difficult to achieve high accuracy in such problems, while the BP neural network, with its strong fault tolerance, self-learning characteristics and nonlinear mapping function, can construct a junction temperature prediction model without pre-determining the specific mathematical relationship between temperature-sensitive electrical parameters and the junction temperature to achieve an accurate junction temperature estimation.

In this paper, VCE, IC and TC are selected as model inputs and junction temperature Tj as output. The BP neural network is trained through forward signal propagation and backward error propagation. During training, network weights and biases are iteratively updated using gradient descent to minimise the mean square error between predicted and actual junction temperatures.

In the forward propagation process, the input signals VCE, IC, and TC are nonlinearly transformed by the implicit layer and passed to the output layer to obtain the predicted value of the junction temperature, Tjp. If there is a deviation between Tjp and the true value, Tj, the error back propagation process is initiated, and the error is apportioned layer-by-layer to each neuron, accordingly, adjusting the weights of each layer ωak (a = 1, 2, ..., a; k = 1, 2, ..., k) and the threshold bc (c = 1, 2, ..., c), so that the network weights and biases are updated in the direction of the fastest decreasing error, and the output error is finally minimised.

The structure of the BP neural network is shown in Figure 3, where fiZ (Z = 0, 1, 2, ..., z) denotes the number of neurons in the hidden layer.

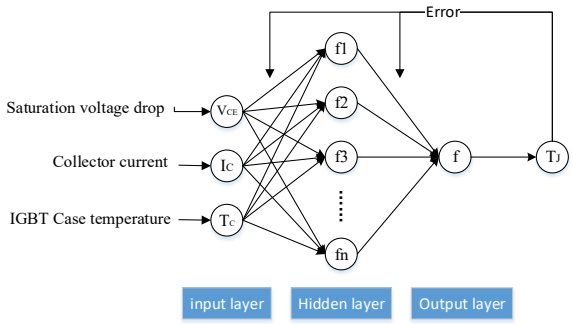

Figure 3. Structure of the BP neural network algorithm

2.2.1 Optimisation of BP Model Parameters Based on Genetic Algorithm

The prediction performance of a BP neural network for IGBT junction temperature estimation is highly dependent on the configuration and coordination of its weights and thresholds. Although BP networks are capable of automatically learning nonlinear mappings from labelled experimental data, the standard BP algorithm is well known for its slow convergence behaviour. In general, increasing training depth can improve model accuracy; however, beyond a certain point, excessive training may degrade generalisation performance, resulting in overfitting.

To address these limitations, a genetic algorithm (GA) is introduced to perform global optimisation of BP neural

network weights and thresholds, thereby constructing a GA-BP-based junction temperature prediction model. This strategy aims to improve regression performance by optimising the initial parameter configuration of the BP neural network. The overall optimisation procedure of the GA-BP model is illustrated in Figure 4.

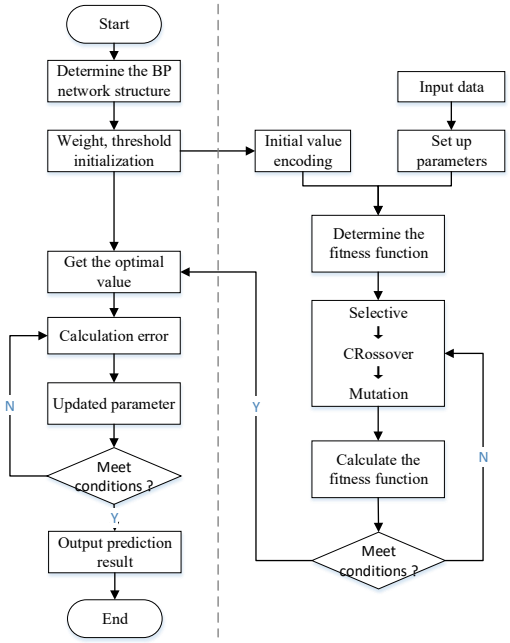

Figure 4. Flow chart of the GA-BP neural network algorithm

For each individual, the encoded weights and thresholds are decoded and used to initialise the BP neural network, which is subsequently trained using the training dataset. The sum of absolute errors between predicted and target outputs is adopted as the fitness value F.

$$F = k(\sum_{i=1}^{m}|x_i - y_i|)$$

where m denotes the number of samples, xi represents the i-th experimental junction temperature, and yi denotes the corresponding predicted value.

2.2.2 Optimisation of LM-based BP Model Parameters

The integration of GA, LM, and BP is motivated by the inherent limitations of conventional BP networks in junction temperature prediction tasks, including slow convergence and susceptibility to local optima. In the proposed hybrid optimisation strategy, GA performs global parameter optimisation, while LM provides subsequent local fine-tuning to improve convergence efficiency.

Initially, GA optimisation is applied to obtain near-optimal initial weights and thresholds for the BP neural network, with a chromosome length of 51 and a population size of 102. Individual performance is evaluated using a fitness function, and individuals with higher fitness are preferentially selected for evolution. Population diversity is maintained through adaptive mutation strategies to avoid premature convergence.

Subsequently, the LM algorithm is employed for local fine-tuning, using the GA-optimised parameters as initial values. By leveraging its approximate second-order convergence characteristics, the LM algorithm rapidly reduces training error. During optimisation, the mean square error (MSE) of the training set is used as the objective function, while the validation set MSE is simultaneously monitored to ensure generalisation capability. The error convergence threshold is set to 0.01, balancing prediction accuracy (within ±1 °C) and training efficiency.

This hybrid strategy effectively combines the global exploration capability of GA with the fast local convergence advantage of LM, resulting in significantly improved model robustness and convergence speed. The overall optimisation flow of the GA-LM-BP neural network is illustrated in Figure 5.

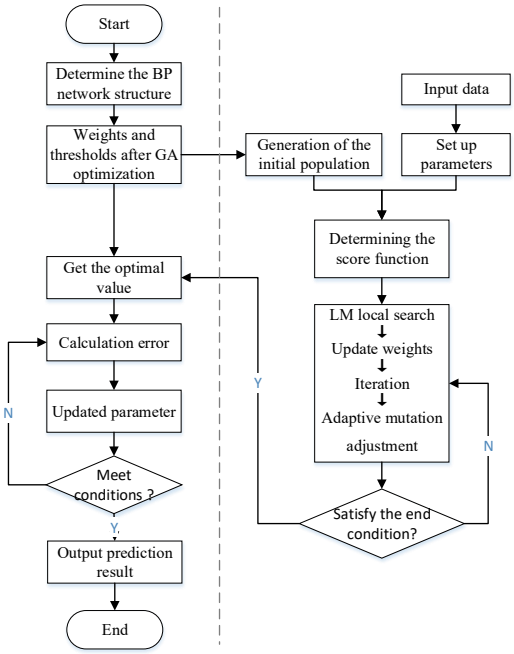

Figure 5 Flow Chart of the GA-LM-BP Neural Network Algorithm

3. Experimental Results and Analyses

3.1 Indicators of prediction error

To quantitatively evaluate the prediction performance of the models, the mean absolute percentage error (δ_{MAP}) and the root mean square error (δ_{RMS}) are adopted as evaluation metrics, defined as follows:

$$\delta_{MAP} = \frac{1}{m}\sum_{i=1}^{m}\left|\frac{x_i - y_i}{y_i}\right|$$

$$\delta_{RMS} = \sqrt{\frac{\sum_{i=1}^{m}(x_i - y_i)^2}{m}}$$

3.2 Data processing and parameterisation

A total of 2250 valid data samples were obtained from the saturation voltage drop experimental platform and divided into training, validation, and test sets at a ratio of 70%:15%:15%. For the GA-LM-BP model, the population size was set to 100, with 10 winning and 10 temporary subpopulations, and the number of iterations was set to 10; for the GA-BP model, the population size was set to 10, with a crossover probability of 0.2 and a mutation probability of 0.1. Figure 6 presents the relationship between saturation voltage drop (VCE) and junction temperature (Tj) under different collector current (IC) conditions.

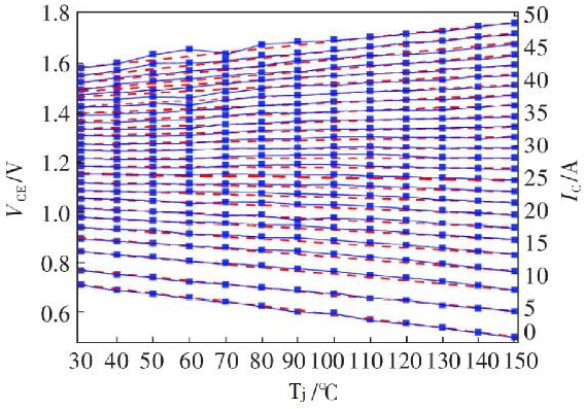

Figure 6. Relationship between Tj and VCE under different IC

As shown in Figure 6, an inflexion point is observed at a collector current of approximately 25 A for the tested module. When the collector current I_C is lower than 25 A, VCE decreases with increasing junction temperature, whereas when I_C exceeds 25 A, V_{CE} increases with increasing junction temperature. In both current intervals, an approximately linear relationship between V_{CE} and T_j is observed. Based on this observed inflexion point, the experimental data are categorised into two current intervals for subsequent analysis: a low-current interval (I_C = 1~25 A) and a high-current interval (I_C = 26~50 A).

3.3 Comparison of Prediction Results

Based on the electrical parameters extracted from the saturation voltage drop experimental platform, the prediction results of the GA-LM-BP model are compared with those of the conventional BP neural network and the GA-BP model. Tables 1 and 2 present the junction temperature prediction results of the three algorithms when the collector current I_C is lower than and higher than 25 A, respectively. Differences in prediction deviations among the three models can be observed under the two current intervals.

Table 1. Prediction Results of Junction Temperature of Three Algorithms at I_C<25A

I_C/A	V_{CE}/V	T_C/℃	Junction temperature experimental /℃	Junction temperature prediction /℃		
				BP	GA-BP	GA-LM-BP
6.00	0.84	75.2	80.00	83.72	86.91	78.53
6.00	0.88	35.6	40.00	42.63	51.65	44.54
8.00	0.90	74.8	80.00	80.82	86.58	74.86
8.00	0.91	55.3	60.00	67.84	74.25	61.71
10.00	0.95	54.5	60.00	66.38	78.73	61.47
10.00	0.97	34.9	40.00	47.09	58.67	40.72
18.00	1.10	112.6	120.00	110.15	111.51	122.33
18.00	1.11	62.7	70.00	74.32	89.77	73.35
24.00	1.22	61.2	70.00	97.24	97.73	71.38
24.00	1.21	32.4	40.00	103.94	108.24	43.59

Table 2. Prediction Results of Junction Temperature of Three Algorithms at IC > 25A

I_C/A	V_{CE}/V	T_C/℃	Junction temperature experimental /℃	Junction temperature prediction /℃		
				BP	GA-BP	GA-LM-BP
28.00	1.30	89.1	100.00	134.05	128.15	117.91
28.00	1.27	49.3	60.00	41.37	47.66	55.18
32.00	1.33	37.2	50.00	47.01	42.82	48.77
32.00	1.37	96.8	110.00	109.52	114.59	113.64
40.00	1.48	52.2	70.00	72.78	72.94	70.45
40.00	1.51	91.9	110.00	110.41	109.06	116.93
44.00	1.54	49.7	70.00	70.18	71.37	69.23
44.00	1.49	10.3	30.00	20.75	22.98	29.29
48.00	1.54	7.8	30.00	24.85	14.41	27.79
48.00	1.65	70.7	100.00	97.22	96.23	97.45

The prediction errors (ΔT_j) of the three algorithms at collector currents below and above 25 A are shown in Figure 7, where E denotes the sample index. Under the low-current condition (I_C < 25 A), the three models exhibit different error distributions, with noticeable variations in error magnitude among individual samples. Under the high-current condition (I_C > 25 A), the prediction errors of the three algorithms show reduced dispersion compared with the low-current interval, while differences among the models remain observable.

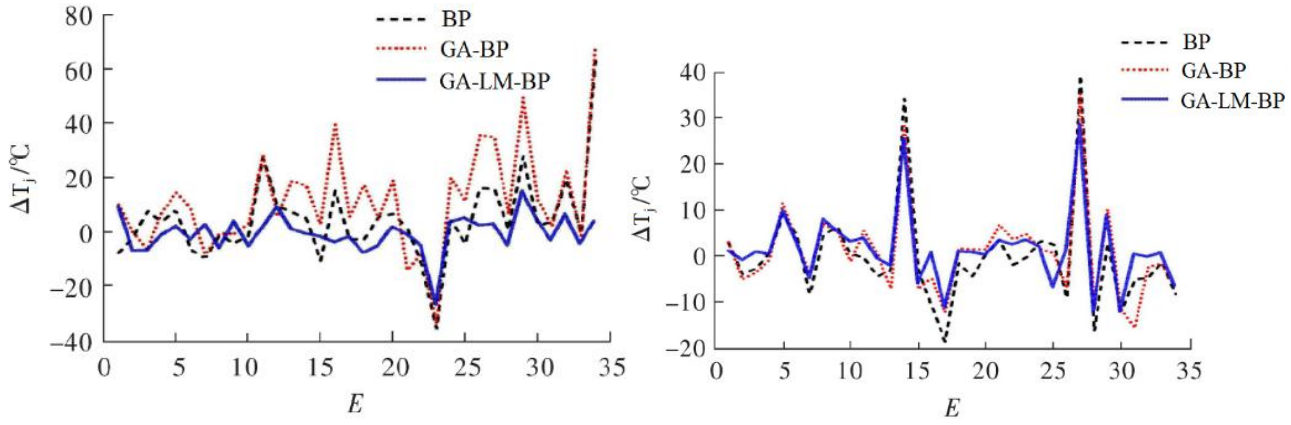

Figure 7. Error Comparison Between the Predicted Value and the Actual Value of the Junction Temperature of Three Algorithms

Figure 8 presents the relative errors ($\Delta\varphi$) of the three algorithms for junction temperature prediction under low-current and high-current conditions. Variations in relative error magnitude can be observed among the three models across different samples. The distributions of relative errors differ between the two current intervals, reflecting the influence of operating conditions on prediction results.

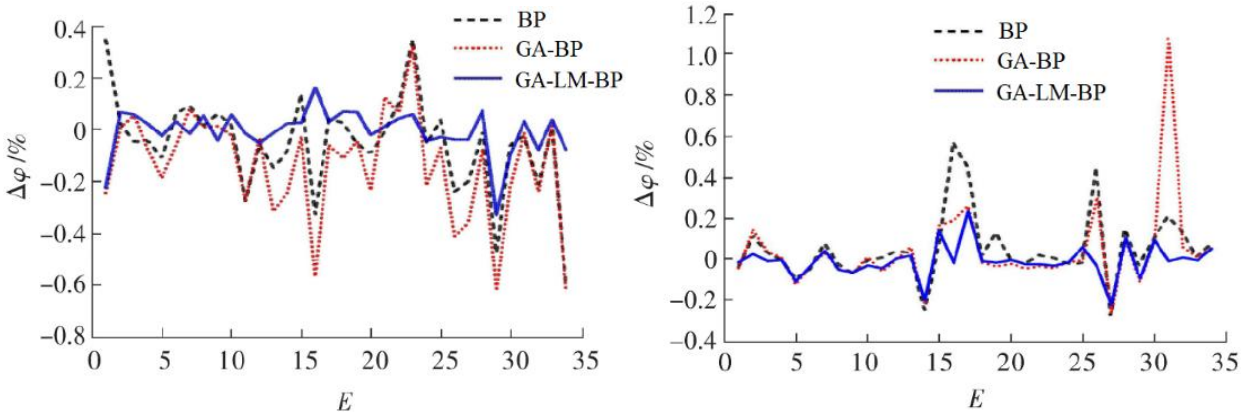

Figure 8. Comparison Of the Relative Error Between the Predicted Value And the Actual Value of the Junction Temperature of Three Algorithms

Table 3 summarises the error metrics of the three algorithms under low-current and high-current conditions. Differences in δ_{MAP} and values among the BP, GA-BP, and GA-LM-BP models can be observed for both operating intervals. The reported error metrics provide a quantitative basis for comparing model performance under different current conditions.

Table 3. Error Data of Three Algorithms

Arithmetic	Working Condition	δ_{RMS}	δ_{MAP}
BP	I_C <25A	15.228	0.138
	I_C >25A	11.992	0.104
GA-BP	I_C <25A	16.624	0.148
	I_C >25A	10.026	0.093
GA-LM-BP	I_C <25A	13.791	0.114
	I_C >25A	7.803	0.062

4. Discussion

This study investigates a data-driven approach for IGBT junction temperature prediction by integrating the genetic algorithm (GA) and the Levenberg–Marquardt (LM) algorithm into a BP neural network framework. Unlike traditional thermal or physics-based models that rely heavily on accurate parameter identification and simplified assumptions, the proposed GA-LM-BP model establishes a direct nonlinear mapping between temperature-sensitive electrical parameters and junction temperature, enabling accurate estimation under varying operating conditions.

The experimental results demonstrate that incorporating GA-based global optimisation effectively alleviates the sensitivity of conventional BP networks to initial parameter settings, while the subsequent introduction of the LM algorithm significantly accelerates local convergence and improves numerical stability. This hybrid optimisation strategy helps explain the differences in prediction error distributions observed among the three models across both low-current and high-current operating regions. In particular, the enhanced performance near the current inflexion point highlights the advantage of combining global exploration with local fine-tuning when dealing with strongly nonlinear electro-thermal coupling characteristics.

From a methodological perspective, the comparative analysis confirms that performance improvements are not solely attributable to increased model complexity, but rather to the complementary roles of GA and LM within the optimisation process. While GA-BP improves prediction accuracy in certain operating intervals, its performance exhibits greater variability, especially under high-current conditions. The GA-LM-BP framework mitigates this issue by refining GA-optimised solutions through LM-based local optimisation, resulting in improved robustness and generalisation capability.

Although the experimental validation in this work is conducted on a single IGBT module rating, the proposed framework is inherently model-agnostic. By retraining the network using temperature-sensitive electrical parameters obtained from other device ratings or package types, the method can be extended to a wide range of IGBT modules.

The primary requirement for such adaptation lies in the availability of representative experimental data rather than modifications to the model structure itself.

It should be noted that the current study focuses on steady-state or quasi-steady operating conditions using experimentally extracted features. Future research may extend this framework to dynamic operating scenarios and explore the integration of temporal learning models or embedded implementation strategies. Nevertheless, the proposed GA-LM-BP approach provides a favourable balance between prediction accuracy, computational complexity, and practical applicability, making it well-suited for real-time junction temperature monitoring in power electronic systems.

5. Conclusion

Accurate estimation of IGBT junction temperature remains a critical challenge in the thermal management of power electronic devices. In this study, a data-driven junction temperature prediction framework was developed based on temperature-sensitive electrical parameters extracted using the TSEP method. By utilising saturation voltage drop, collector current, and case temperature as input features, a BP neural network–based prediction model was established, and hybrid optimisation strategies were applied to enhance model training and convergence characteristics.

Experimental results obtained under different current conditions demonstrate that the proposed framework is capable of providing reliable junction temperature predictions across both low-current and high-current operating regions. The comparative results among different optimisation strategies indicate that incorporating global and local optimisation techniques into BP-based models offers a feasible approach for improving prediction consistency under varying operating conditions.

Although the experimental validation in this work was conducted using a specific IGBT module, the proposed GA-LM-BP framework is model-agnostic and can be extended to other IGBT ratings or package types through retraining with corresponding experimental datasets. Such adaptation primarily depends on the availability of representative temperature-sensitive electrical measurements rather than modifications to the model structure. Future work will focus on the implementation of the proposed model on FPGA-based digital driver platforms, aiming to enable real-time, online junction temperature monitoring in practical power electronic applications.

Funding: This work was supported by the Natural Science Basic Research Program of Shaanxi under Grant Number [No. 2024JC-YBQN-0603]; Scientific Research Program Funded by Shaanxi Provincial Education Commission under Grant Number [NO. 23JK1602]; Chancellor's Fund Research Projects by Xian Siyuan University under Grant Number [XASYB24ZD02].

Conflicts of Interest: The authors declare no conflicts of interest related to this study..

Ethics Statement and Informed Consent Statement: Not applicable.

Informed Consent Statement: Not applicable.

Acknowledgements: The authors would like to thank the participating students and staff for their valuable time and contributions. We also acknowledge the support of the university’s research office for facilitating data collection.

Data Availability Statement: All data generated or analysed during this study are openly accessible.

References

[1] Morel, C.; Morel, J.Y. Power semiconductor junction temperature and lifetime estimations: A review. Energies 2024, 17, 4589. https://doi.org/10.3390/en17184589.

[2] Wang, W.; Xiang, L.; Zhao, G. Application review of IGBT power module cooling system. Electric Drive for Locomotives 2022, 6, 130–137. https://doi.org/10.13890/j.issn.1000-128X.2022.06.019.

[3] Falck, J.; Felgemacher, C.; Rojko, A.; et al. Reliability of power electronic systems: An industry perspective. IEEE Industrial Electronics Magazine 2018. https://doi.org/10.1109/MIE.2018.2825481.

[4] Dugal, F.; Ciappa, M. Study of thermal cycling and temperature ageing on PbSnAg die attach solder joints for high power modules. Microelectronics Reliability 2014, 54, 1856–1861. https://doi.org/10.1016/j.microrel.2014.08.001.

[5] Kang, Y.; Dang, L.; Yang, L.; et al. Research progress in failure mechanism and health state evaluation index system of welded IGBT power modules. Electronics 2023, 12, 3527. https://doi.org/10.3390/electronics12153248.

[6] Zhao, S.; Yang, X.; Wu, X.; et al. Investigation on fatigue mechanism of solder layers in IGBT modules under high temperature gradients. Microelectronics Reliability 2023, 141, 114901. https://doi.org/10.1016/j.microrel.2023.114901.

[7] Farhadi, M.; Vankayalapati, B.T.; Sajadi, R.; Akin, B. AC power cycling test setup and condition monitoring tools for SiC-based traction inverters. IEEE Transactions on Transportation Electrification 2023. https://doi.org/10.48550/arXiv.2307.10110.

[8] Zhang, B.; Gao, Y. IGBT reliability analysis of photovoltaic inverter with reactive power output capability. Microelectronics Reliability 2023, 147, 115073. https://doi.org/10.1016/j.microrel.2023.115073

[9] Shi, Y.; Liu, J.; Ai, Y.; et al. Dynamic IGBT three-dimensional thermal network model considering base solder degradation and thermal coupling between IGBT chips. IEEE Transactions on Transportation Electrification 2022, 9, 2994–3011. https://doi.org/10.1109/TTE.2022.3228440

[10] Lu, Y.; Xiang, E.; Jin, Y.; et al. A 3-D temperature-dependent thermal model of IGBT modules for electric vehicle application considering various boundary conditions. IEEE Journal of Emerging and Selected Topics in Power Electronics 2024, 12, 5463–5475. https://doi.org/10.1109/JESTPE.2024.3355715

[11] Zhang, X.; Mu, W.; Lv, C.; et al. A thermal network model for monitoring the IGBT chip solder degradation based on feedback PI control. Microelectronics Reliability 2022, 133, 114617. https://doi.org/10.1016/j.microrel.2022.114617.

[12] Sathik, M.H.M.; Jet, T.K.; Kandasamy, K.; et al. Online junction temperature estimation of IGBT modules for space vector modulation-based inverter system. Proceedings of SPEEDAM 2016. https://doi.org/10.1109/SPEEDAM.2016.7525975.

[13] Baker, N.; Munk-Nielsen, S.; Iannuzzo, F.; et al. IGBT junction temperature measurement via peak gate current. IEEE Transactions on Power Electronics 2016, 31, 3784–3793. https://doi.org/10.1109/TPEL.2015.2464714

[14] Yang, Y.; Zhang, P. A novel converter-level IGBT junction temperature estimation method based on the bus voltage ringing. IEEE Transactions on Power Electronics 2021, 37, 4553–4563. https://doi.org/10.1109/TPEL.2021.3119700

[15] Zhang, W.; Qi, L.; Tan, K.; et al. IGBT junction temperature estimation using a dynamic TSEP independent of wire bonding faults. IEEE Transactions on Power Electronics 2022, 38, 5323–5334. https://doi.org/10.1109/TPEL.2022.3230790

[16] Yang, Y.; Ding, X.; Zhang, P. A novel junction temperature estimation method independent of bond wire degradation for IGBT. IEEE Transactions on Power Electronics 2023, 38, 10256–10268. https://doi.org/10.1109/TPEL.2023.3274126

[17] Arya, A.; Chanekar, A.; Verma, A.; et al. Multiple points measurement-based junction temperature estimation of IGBT module. IEEE Journal of Emerging and Selected Topics in Power Electronics 2023, 11, 3457–3467. https://doi.org/10.1109/JESTPE.2023.3239111

[18] Wei, X.; Yao, B.; Zhang, Y.; et al. Online junction temperature estimation for IGBT devices through knee voltage. IEEE Transactions on Power Electronics 2024. https://doi.org/10.1109/TPEL.2024.3439250

[19] Wei, W.; Hu, Y.; Liu, S.; et al. Online junction temperature detection for IGBT using voltage rise time. IEEE Transactions on Electron Devices 2025. https://doi.org/10.1109/TED.2025.3574125

[20] Shi, Y.; Zhang, B.; Kang, J.; et al. An IGBT junction temperature estimation method based on turn-off maximum diC/dt with decoupling load current. IEEE Transactions on Power Electronics 2024. https://doi.org/10.1109/TPEL.2024.3449551

[21] Lamuadni, B.; El Bouayadi, R.; Amine, A.; et al. Design and development of a measurement system dedicated to estimating the junction temperature of insulated gate bipolar transistor modules. International Journal of Engineering Research in Africa 2022, 60, 89–106. https://doi.org/10.4028/p-z9wh2k

[22] Morel, C.; Morel, J.Y. Power semiconductor junction temperature and lifetime estimations: A review. Energies 2024, 17, 4589. https://doi.org/10.3390/en17184589

[23] Liu, L.; Peng, Q.; Jiang, H.; et al. BP neural network for non-invasive IGBT junction temperature online detection. Microelectronics Reliability 2023, 141, 114882. https://doi.org/10.1016/j.microrel.2022.114882

[24] Li, L.; Liu, J.; Tseng, M.L.; et al. Accuracy of IGBT junction temperature prediction: An improved sailfish algorithm to optimise support vector machine. IEEE Transactions on Power Electronics 2024, 39, 6864–6876. https://doi.org/10.1109/TPEL.2024.3370690

[25] Zhou, C.; Gao, B.; Yang, H.; et al. Junction temperature prediction of insulated-gate bipolar transistors in wind power systems based on an improved honey badger algorithm. Energies 2022, 15, 7366. https://doi.org/10.3390/en15197366

[26] Li, J.; Li, L.; Liu, Y. Nondestructive and accurate prediction of IGBT junction temperature in wind power converters: Based on IDMOA-ELM prediction method. Nondestructive Testing and Evaluation 2025, 40, 2369–2399. https://doi.org/10.1080/10589759.2024.2378908

[27] Wang, J.; Wang, X. Junction temperature prediction method of discrete IGBT based on PIN temperature. Proceedings of the 2025 5th International Conference on Mechanical, Electronics and Electrical and Automation Control (METMS) 2025, 135–140.

[28] Tan, S.; Wei, B.; Vasquez, J.C.; et al. Junction temperature estimation technologies of IGBT modules in converter-based applications. Proceedings of IECON 2023—49th Annual Conference of the IEEE Industrial Electronics Society 2023, 1–6.

[29] Ma, T.; Yan, B.; Liu, B.; et al. Application of IGBT junction temperature estimation in hybrid electric vehicles. Microelectronics Reliability 2025, 167, 115629. https://doi.org/10.1016/j.microrel.2025.115629.

[30] Su, C.; Jiang, W.; Huang, Z. IGBT junction temperature estimation based on external parameters of multiple drive devices in a practical industrial scenario. International Journal of Circuit Theory and Applications 2025, 53, 5379–5393. https://doi.org/10.1002/cta.4391